Ultrastructural localization of calcium in the organic acid secreting trichomes of chickpea (*Cicer arietinum*)

MARK D. LAZZARO[1] AND WILLIAM W. THOMSON[2]

Department of Botany and Plant Science, University of California, Riverside, CA 92521, U.S.A

Received March 31, 1992

LAZZARO, M. D., and THOMSON, W. M. 1992. Ultrastructural localization of calcium in the organic acid secreting trichomes of chickpea (*Cicer arietinum*). Can. J. Bot. **70**: 2319–2325.

In the organic acid secreting trichomes of chickpea (*Cicer arietinum* L.), calcium is localized in the stalk and head cells using pyroantimonate and X-ray microanalysis. Light calcium deposits are present in the endoplasmic reticulum, mitochondria, and cytoplasm of the stalk and head cells and in the cell walls of the stalk cells. Dense calcium deposits are present in the vacuoles of stalk and head cells and within the plasmodesmata between stalk cells. In the head cells, heavy calcium deposits are present in small, secretory vesicles that fuse with the plasma membrane. In addition, calcium deposits are localized in the cell wall space around the head cells, in the secretion chamber, and in collected secretions. These observations suggest that secretion from the head cells occurs predominantly through an exocytotic, vesicular pathway. We conclude that once secreted, calcium diffuses through the walls to the collecting chamber and subsequently through the cuticular pores into the secretion droplet.

Key words: calcium secretion, *Cicer arietinum*, pyroantimonate, secretory vesicles, trichome.

LAZZARO, M. D., et THOMSON, W. M. 1992. Ultrastructural localization of calcium in the organic acid secreting trichomes of chickpea (*Cicer arietinum*). Can. J. Bot. **70** : 2319–2325.

En utilisant le pyroantimonate et la micro-analyse aux rayons X, les auteurs ont examiné les trichomes qui secrètent des acides organiques chez le *Cicer arietinum* L. et ils montrent que du calcium se retrouve dans le pied ainsi que dans les cellules terminales. De faibles dépôts de calcium se retrouvent dans le réticulum endoplasmique, les mitochondries et le cytoplasme du pied et des cellules terminales, ainsi que dans les parois des cellules du pied. Les forts dépôts de calcium sont localisés dans les vacuoles des cellules podiales et terminales, ainsi qu'à l'intérieur des plasmodesmes entre les cellules podiales. Dans les cellules terminales, on retrouve de forts dépôts de calcium dans de petites vésicules secrétrices qui se fusionnent avec la plasmalemme. De plus, les dépôts de calcium sont localisés dans l'espace de la paroi cellulaire autour des cellules terminales, dans la chambre de secrétion et dans les secrétions récoltées. Ces observations suggèrent que la secrétion par les cellules terminales s'effectiue surtout via un chemin vésiculaire exocytotique. Les auteurs concluent qu'une fois secrété, le calcium diffuse à travers les parois de la chambre d'accumulation et subséquemment à travers les pores cuticulaires pour former la gouttelette de secrétion.

Mots clés : secrétion de calcium, *Cicer arietinum*, pyroantimonate, vésicules de secrétion, trichome.

[Traduit par la rédaction]

Introduction

The multicellular secretory trichomes of chickpea (*Cicer arietinum* L.) have three long stalk cells topped by four tiers of head cells with an outer subcuticular secretion chamber. The secretion droplet, containing primarily malate and oxalate (Rembold and Weigner 1990; Lauter and Munns 1986), collects on the tip of the trichome (Lazzaro and Thomson 1989; Schnepf 1965). The pH of the secretion is 1.0 or less (Lauter and Munns 1986), and this low pH is thought to prevent insect herbivory (Rembold and Weigner 1990). Lauter and Munns (1986) found that in addition to organic acids and hydrogen, the secretory fluid contains some chloride, potassium, magnesium, and calcium. This study uses the pyroantimonate precipitation technique to localize calcium to assess the possible pathways for the movement and secretion of calcium by these trichomes.

Materials and methods

Secretory trichomes from leaves of *C. arietinum* L. cv. UC5 were treated with potassium pyroantimonate using a method modified from Slocum and Roux (1982). Sodium phosphate buffer (0.1 M) was titrated to pH 8.2 with 1.0 M NaOH and then heated to 80–90°C. Potassium pyroantimonate was added (2% w/v) and heated at 80–90°C for 30 min. The solution was cooled to room temperature, titrated to pH 7.6 using 1.0 M HCl, and filtered through a Gelman Acrodisc filter (0.22 μm) immediately before use. This solution was used as a buffer to make the glutaraldehyde, paraformaldehyde, and osmium tetroxide fixatives. For controls, buffer without potassium pyroantimonate was used to make the fixatives. Leaf tissue was cut into small pieces in buffered 2% glutaraldehyde and 2.5% paraformaldehyde (Karnovsky 1965) with 0.1% tannic acid and fixed for 2 h. Tissue was then rinsed in buffer for 15 min and postfixed in buffered 1% OsO_4 for 18 h at 4°C. Tissue was then rinsed in three changes of buffer for 30 min each, with the final rinse being in buffer that did not contain potassium pyroantimonate for both the treated and control tissues. Material was then dehydrated through a graded acetone series and infiltrated with Spurr's resin (Spurr 1969) by dropwise addition. Thin sections (90 nm) were cut with glass or diamond knives and examined unstained, except for the section in Fig. 10, which was post-stained with aqueous uranyl acetate and lead citrate. Sections were examined with a Philips 400 transmission electron microscope (TEM) at 60 or 80 kV.

To see if secretions collected from the trichomes reacted with pyroantimonate, 100 μL of either collected secretions, 3.75 mM calcium carbonate in dilute HCl, or distilled water were added to 100 μL of the 2% potassium pyroantimonate fixative described above. The $CaCO_3$ and dH_2O were included as controls, and this method was modified from Wick and Hepler (1980). After 20 h at 22°C, these mixtures were centrifuged at 10 000 × *g* for 4 min. Pellets were present in the tubes of secretion and $CaCO_3$ but were absent in tubes of dH_2O. These pellets were prepared for electron microscopy as described above.

The elemental composition of electron-dense deposits was deter-

[1]Present address: Department of Biology, University of California, Riverside, CA 92521, U.S.A.

[2]Author to whom all correspondence should be addressed.

TABLE 1. X-ray microanalysis of calcium antimonate deposits

Cell type	K K_α	Sb L_α	Sb L_β	Ca K_α	Ca K_β
Stalk cell vacuoles					
Treated	1.66±0.70 ns	18.77±3.61*	4.98±2.23*	9.67±4.76 ns	2.02±1.20 ns
Control	0.90±0.24	0.28±0.39	0.46±0.36	0.88±0.10	0.14±0.20
Stalk cell plasmodesmata					
Treated	0 ns	3.07±0.29*	1.37±0.19*	2.76±0.09*	0.60±0.06 ns
Control	0.21±0.30	0.71±0.14	0	0.86±0.17	0.23±0.33
Head cell vesicles					
Treated	0 ns	6.98±1.23*	3.46±0.64*	7.62±0.83*	1.07±0.76 ns
Control	0.49±0.34	0.98±0.25	0	1.27±0.05	0.26±0.36
Head cell vacuole					
Treated	0 ns	5.03±1.85*	2.85±0.96*	5.22±2.57 ns	0.93±0.39*
Control	0.24±0.34	0.48±0.68	0	0.93±0.70	0
Secretion chamber					
Treated	0.15±0.21 ns	7.85±1.53*	3.80±1.01*	5.73±1.33*	1.34±0.44*
Control	0.42±0.30	0	0	0.64±0.47	0
Secretions					
Treated	4.13±0.10*	3.00±0.22*	1.50±0.07*	3.14±0.45*	0.91±0.10*
Control	0	0	0	0	0.13±0.19
$CaCO_3$ standard					
Treated	4.39±0.56*	2.35±0.14*	0.90±0.09*	2.75±0.16*	0.51±0.39 ns
Control	0	0	0	0	0.13±0.19
Secretions vs. $CaCO_3$ standard	ns	*	*	ns	ns

NOTE: Values are means ± SD (n = 3). Counts per second measured for potassium, antimony, and calcium in antimonate-treated and control tissue and in test-tube precipitates.

*Significant difference at $p < 0.05$ between treated and control tissue using a pairwise T-test (t = 2.78).

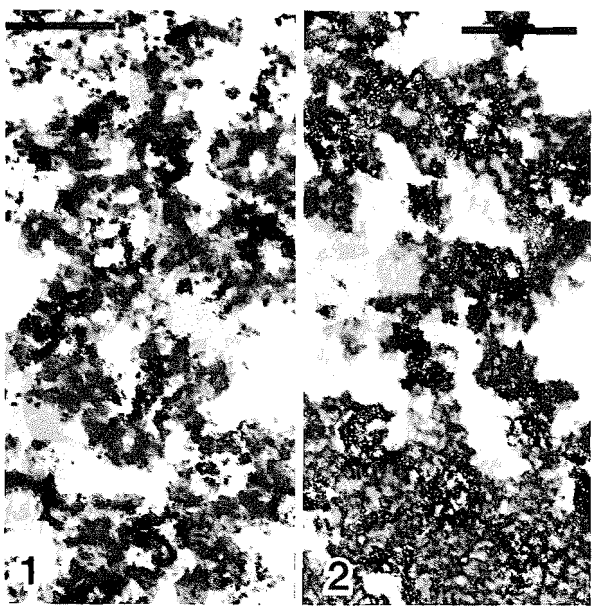

FIG. 1. The test-tube reaction of collected secretions with potassium pyroantimonate formed electron-dense deposits similar to those observed within the trichome cells. FIG. 2. The test-tube reaction of $CaCO_3$ with potassium pyroantimonate formed electron-dense deposits similar to the deposits formed from reacting collected secretions with pyroantimonate and those observed in the trichome cells. Scale bars = 1.0 μm.

mined using X-ray microanalysis. Thick sections (350 nm) were analyzed with an EDAX 9100 and a Philips 400 TEM at 60 kV, with a 0.5 μm spotsize at 24° tilt. Counts per second were calculated by the EDAX computer using the EDAX semiquantitative program. Counts were calculated for potassium (K_α = 3.316 keV), antimony (L_α = 3.604 keV, L_β = 3.843 keV), and calcium (K_α = 3.693 keV, K_β = 4.014 keV), using a band width of 0.50 keV to avoid peak overlap. Background was subtracted by the EDAX semiquantitative program using a segmented Kramer Law fit that also corrected for detector efficiency. Reported counts are averages of three replications that were taken from different regions within the same trichome. The average count time for each measurement was 112 s.

Results

Suspected calcium antimonate precipitates in the trichomes were verified with X-ray microanalysis and counts per second were calculated for antimony, calcium, and potassium. For controls, the same cellular regions or similar electron-dense deposits were analyzed with X-ray microanalysis. In all cases, the counts for antimony in treated tissues were significantly higher than counts measured in controls (Table 1). Also, in all cases except the stalk cell vacuoles, the counts for calcium were significantly higher in treated tissues than counts measured in controls. We tested for potassium with X-ray microanalysis to determine whether the observed deposits were formed from calcium reacting with antimonate or were just deposits of potassium antimonate applied to the tissue, and in all cases, we found no significant differences in measured counts for potassium in treated tissue compared with controls (Table 1). Therefore, we concluded that the observed precipitates in the secretory trichomes resulted from *in situ* calcium reacting with antimonate (Table 1).

The precipitates formed from the reactions of collected secretion or the $CaCO_3$ standard with antimonate were also analyzed with X-ray microanalysis. As a control, distilled water was added to antimonate, but since no precipitate was formed, microanalysis was performed on thick sections of Spurr's resin where the precipitate should have been. The measured counts for antimony and calcium, as well as potassium, were significantly higher than counts in the control for

FIG. 3. In treated stalk cells, calcium antimonate deposits were present in the vacuoles (*v*) and mitochondria (*m*). Scale bar = 1.0 μm. FIG. 4. Stalk cells from controls lacked electron-dense deposits. Scale bar = 1.0 μm. FIG. 5. At higher magnification, dense calcium antimonate deposits were observed in the stalk cell vacuoles (*v*), and lighter deposits were observed in the lateral cell walls (*w*), cytoplasm, and ER. Scale bar = 1.0 μm. FIG. 6. Light calcium antimonate deposits were present in the transverse cell walls between stalk cells (*w*), and heavy deposits were within the lumens of the plasmodesmata, which connected adjacent stalk cells (arrows). Scale bar = 0.5 μm. FIG. 7. The transverse walls and connecting plasmodesmata of control stalk cells did not contain electron-dense deposits. Scale bar = 0.5 μm.

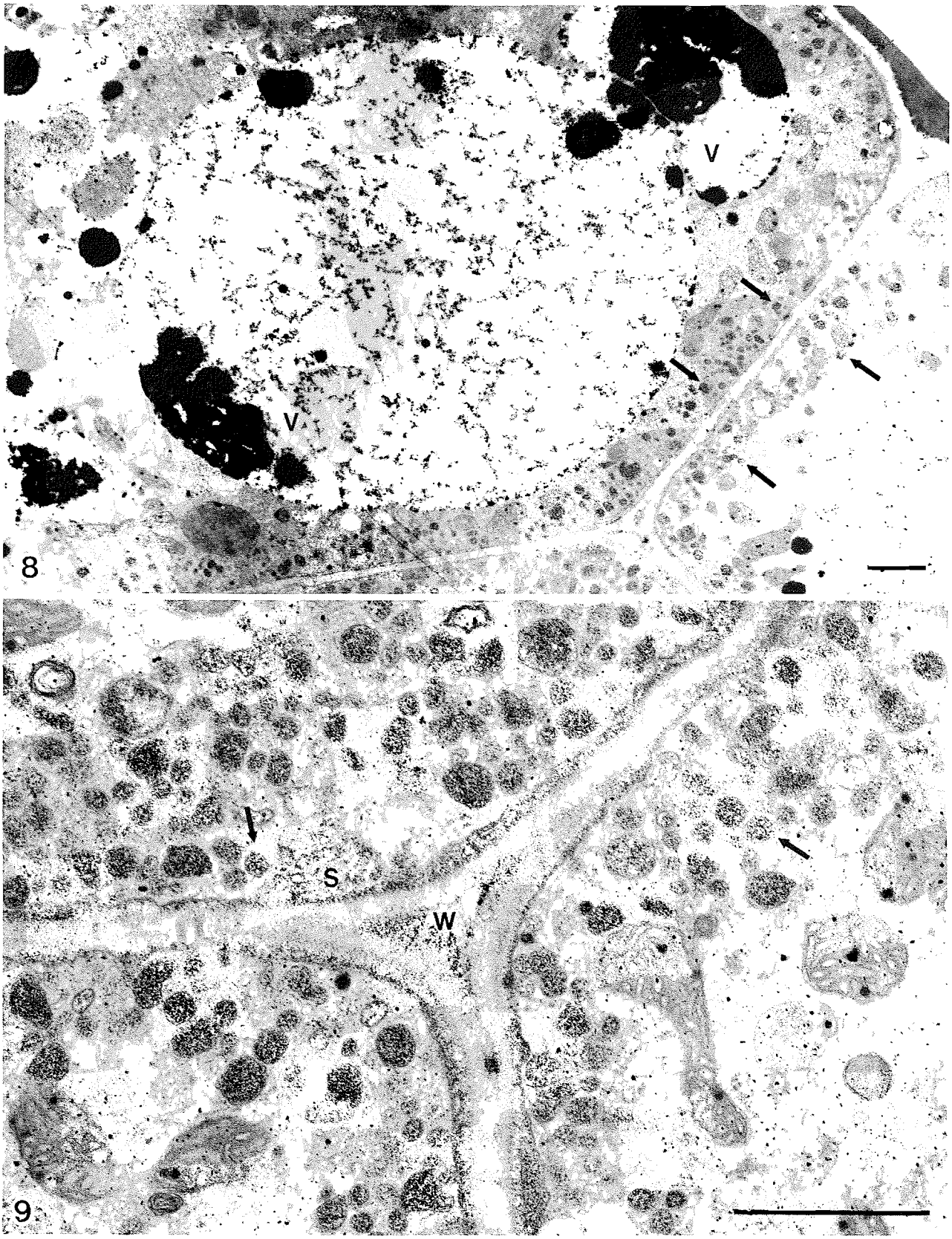

FIG. 8. The vacuoles of treated head cells contained large calcium antimonate deposits (*v*), and deposits were also present within vesicles that formed a layer along the plasma membrane (arrows). FIG. 9. Calcium antimonate deposits were present within vesicles that formed a layer along the periphery of the head cells (arrows). In addition, deposits were present in the cell walls (*w*) and extracellular space (*s*) and within the mitochondrial cristae, cytoplasm, and ER. Scale bars = 1.0 μm.

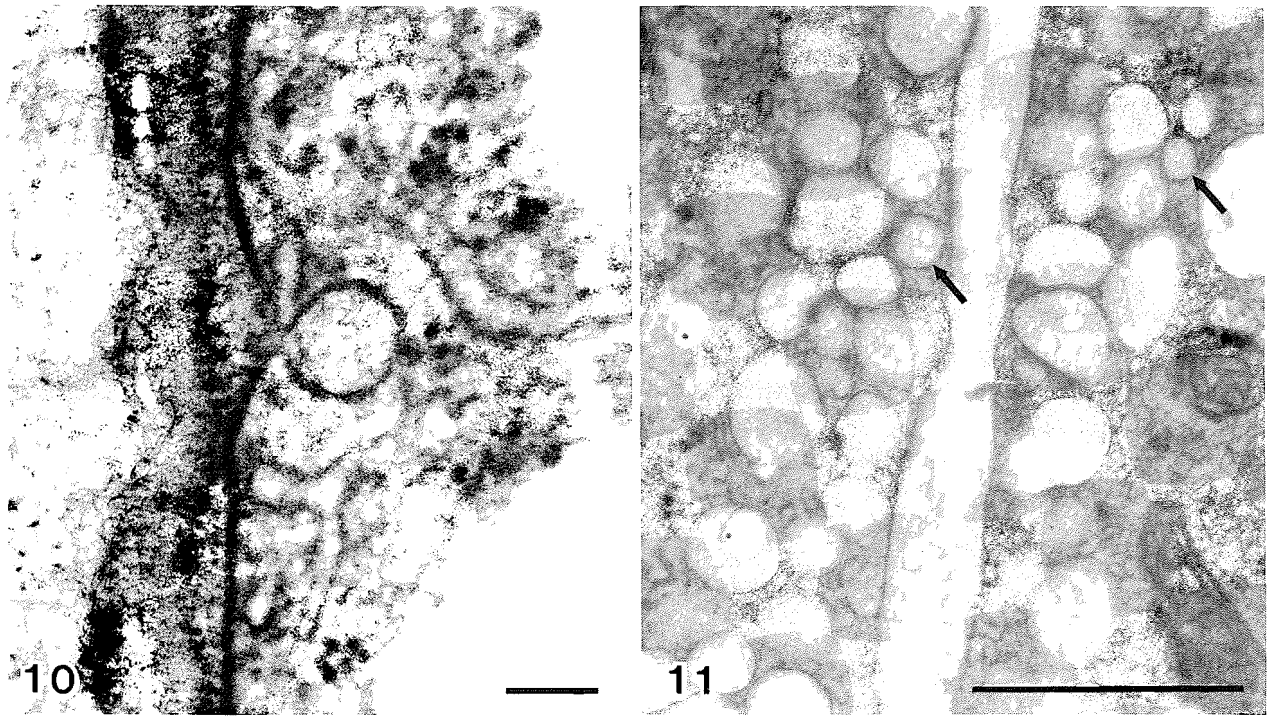

FIG. 10. Light calcium antimonate precipitates were present within secretory vesicles fusing with the plasma membrane, whereas heavier precipitates were present in the extracellular space at the fusion site. Scale bar = 0.1 μm. FIG. 11. Head cells from the control lacked electron-dense deposits in the mitochondria, ER, and cytoplasm, as well as in the secretory vesicles (arrows) and cell wall. Scale bar = 1.0 μm.

both secretions and the standard (Table 1). In addition, there was no significant difference between secretions and the standard for measured counts of calcium or potassium, whereas measured counts for antimony were significantly higher in secretions compared with the standard (Table 1). Ultrastructurally, the calcium antimonate precipitate that formed from the reaction of collected secretion with pyroantimonate (Fig. 1) was similar to the calcium antimonate precipitate formed from the reaction of the calcium carbonate standard with pyroantimonate (Fig. 2). In addition, both of these precipitates were similar to the electron-dense deposits present in the cells of treated trichomes.

In the secretory trichomes, calcium antimonate precipitates were observed in the vacuoles and mitochondria of treated stalk cells (Fig. 3), whereas such deposits were absent in the stalk cells of controls (Fig. 4). Calcium antimonate precipitates were also present in the lateral walls, cytoplasm, and endoplasmic reticulum (ER) of the stalk cells, although the deposition was lighter than that observed in the vacuoles (Fig. 5). The plasmodesmata in the walls between the stalk cells contained dense calcium antimonate precipitates in treated tissue (Fig. 6). These deposits were inside the lumen of the plasmodesmata and often occurred in the median nodules (Fig. 6). The transverse cell walls around these plasmodesmata contained light calcium antimonate precipitates (Fig. 6). The transverse walls and connecting plasmodesmata in controls lacked electron-dense precipitate (Fig. 7).

In the head cells of the secretory trichomes, dense calcium antimonate deposits were present in the vacuoles (Fig. 8), and light deposits were present in the ER, cytoplasm, and within the mitochondrial cristae of the head cells (Fig. 9). Light deposits were also present within numerous vesicles along the periphery of the head cells, as well as in the extracellular space and cell wall (Fig. 9). The peripheral vesicles were observed fusing with the plasma membrane (Fig. 10). Electron-dense deposits were absent in the head cells of control tissue (Fig. 11).

The subcuticular chamber at the top of the secretory trichomes contained calcium antimonate precipitates in treated tissue, and these precipitates were present at the secretory pores that perforated the cuticle (Fig. 12). In addition, calcium antimonate precipitates were present in the extracellular space around the head cells beneath the secretory chamber (Fig. 12). At higher magnification, calcium antimonate deposits were observed within cytoplasmic vesicles in the head cells beneath the secretory chamber (Fig. 13). The secretory chamber of control trichomes lacked electron-dense deposits, although a fine granular matrix was present (Fig. 14).

Discussion

In a critical review on the feasibility of using the antimonate precipitation technique to localize calcium at the subcellular level, Wick and Hepler (1982) noted that the technique has been subjected to a variety of criticisms (for example, Van Iren et al. 1979). Nevertheless, they concluded that antimonate can be used validly for the localization of exchangeable or loosely bound cellular calcium if careful attention is paid to the method of tissue preparation (Wick and Hepler 1982). In the same volume, Slocum and Roux (1982) showed that the incorporation of tannic acid in the fixative increased the retention of calcium and decidedly improved the specificity for calcium and the spatial definition of the precipitate.

Using the improved method of Slocum and Roux (1982) and X-ray microanalysis, we found that the subcellular distribution of calcium antimonate in stalk and head cells was similar to patterns reported in other plant cells (Slocum and Roux 1982,

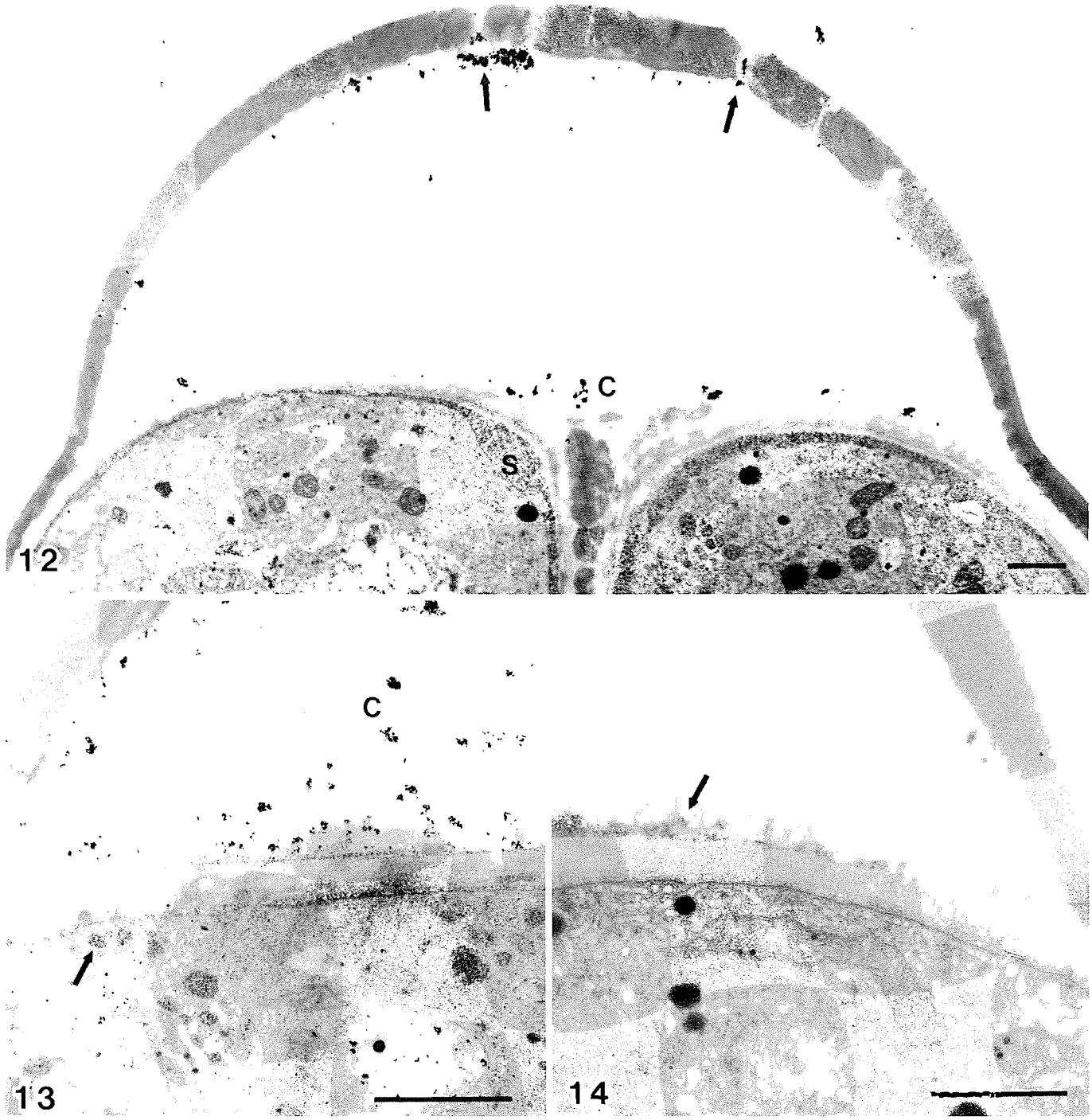

FIG. 12. The subcuticular secretory chamber (*c*) and the pores in the cuticle (arrows) contained calcium antimonate deposits. In addition, deposits were present in the extracellular space beneath the chamber (*s*). FIG. 13. At higher magnification, deposits were observed in the secretory chamber (*c*) and within vesicles in the head cells adjacent to the secretory chamber (arrow). FIG. 14. The secretory chamber in the control lacked electron-dense deposits, although a fine granular matrix was present (arrow). Scale bars = 1.0 μm.

Wick and Hepler 1982), including phloem cells of chickpea (Arsanto 1986). In general, calcium antimonate precipitates occurred in the ER, mitochondria, and cell walls. Heavy deposits were found in the vacuoles and, as suggested by Hepler and Wayne (1985), may be indicative of the vacuole's function in sequestering calcium from the cytoplasm. Heavy deposits were also present in the plasmodesmata in the transverse walls of the stalk cells, which could relate to callose formation, since calcium is reported to affect callose deposition (Robards and Lucas 1990). However, since no ultrastructural evidence for callose was observed, we suggest calcium may be involved in plasmodesmatal function, which has been implied by Robards and Lucas (1990), or the deposits may result from calcium moving between the stalk cells through the plasmodesmata.

In addition, we found calcium antimonate within the vesicles in the head cells. These vesicles occur in large numbers along

the cell periphery, and we assume that these vesicles are secretory, rather than endocytotic, because of the secretory nature of the trichome. Also, fusion of the vesicles with the plasma membrane was observed. The concentration of calcium in collected secretions is only about 1.0 mM (M. D. Lazzaro and W. W. Thomson, unpublished data) and is substantially less than the concentrations of the anions malate (444 mM), oxalate (174 mM), and chloride (231 mM) in secretions (Lauter and Munns 1986). We know of no direct way to localize malate or small quantities of oxalate at the ultrastructural level. However, if we assume that the mechanism for calcium secretion is coupled to that for malate and oxalate, then an exocytotic, vesicular mode of secretion may predominate in these trichomes. In addition, the occurrence of calcium with oxalate is common in plant cells, especially as calcium oxalate crystals (Franceschi and Horner 1980), and in fact, calcium oxalate crystals are present in the cell wall space around the head cells in older trichomes (Lazzaro and Thomson 1989). Calcium antimonate precipitates were also present in the subcuticular secretory chamber, as well as in the cuticular pores, suggesting that secretions collect in this chamber and exude out through the pores in the cuticle to collect in a droplet on the tip of the trichome. This mechanism has been proposed previously for these trichomes (Lazzaro and Thomson 1989; Schnepf 1965) and occurs commonly in plant secretory hairs (Fahn 1988).

In summary, the observed calcium antimonate precipitates suggest that calcium is secreted via vesicular fusion into the extracellular space around the head cells and then diffuses through the cell wall space to the secretory chamber and through the cuticular pores into the secretion droplet.

Acknowledgements

We thank Dr. Kathryn A. Platt for her input on research ideas. This work is supported by National Science Foundation grant DCB-8919064 to William W. Thomson and is part of the Ph.D. dissertation of Mark D. Lazzaro.

Arsanto, J. P. 1986. Ca^{+2} binding sites and phosphatase activities in sieve element reticulum and P-protein of chickpea phloem. A cytochemical and X-ray microanalysis survey. Protoplasma, **132**: 160–171.

Fahn, A. 1988. Secretory tissues in vascular plants. New. Phytol. **108**: 229–257.

Franceschi, V. R., and Horner, H. T. 1980. Calcium oxalate crystals in plants. Bot. Rev. **46**: 361–427.

Hepler, P. K., and Wayne, R. O. 1985. Calcium and plant development. Annu. Rev. Plant Physiol. **36**: 397–439.

Karnovsky, M. J. 1965. A formaldehyde–glutaraldehyde fixative of high osmolarity for use in electron microscopy. J. Cell Biol. **27**: 137A–138A.

Lauter, D. J., and Munns, D. N. 1986. Water loss via the glandular trichomes of chickpea (*Cicer arietinum* L.). J. Exp. Bot. **37**: 640–649.

Lazzaro, M. D., and Thomson, W. W. 1989. Ultrastructure of organic acid secreting trichomes of chickpea (*Cicer arietinum*). Can. J. Bot. **67**: 2669–2677.

Rembold, H., and Weigner, C. 1990. Chemical composition of chickpea, *Cicer arietinum*, exudate. Z. Naturforsch. Sect. C Biosci. **45**: 922–923.

Robards, A. W., and Lucas, W. J. 1990. Plasmodesmata. Annu. Rev. Plant Physiol. Plant Mol. Biol. **41**: 369–419.

Schnepf, E. 1965. Licht- und elektronenmikroskopische Beobachtungen an den Trichom–Hydathoden von *Cicer arietinum*. Z. Pflanzenphysiol. **53**: 245–254.

Slocum, R. D., and Roux, S. J. 1982. An improved method for the subcellular localization of calcium using a modification of the antimonate precipitation technique. J. Histochem. Cytochem. **30**: 617–629.

Spurr, A. R. 1969. A low viscosity epoxy resin embedding medium for electron microscopy. J. Ultrastruct. Res. **26**: 31–43.

Van Iren, F., Van Essen-Joolen, L., Van der Duyn Schouten, P., Boers – Van der Sluijs, P., and de Bruijn, W. C. 1979. Sodium and calcium localization in cells and tissues by precipitation with antimonate: a quantitative study. Histochemistry, **63**: 273–294.

Wick, S. M., and Hepler, P. K. 1980. Localization of Ca^{2+}-containing antimonate precipitates during mitosis. J. Cell Biol. **86**: 500–513.

Wick, S. M., and Hepler, P. K. 1982. Selective localization of intracellular Ca2+ with potassium antimonate. J. Histochem. Cytochem. **30**: 1190–1204.